Misalignment estimation of a lightweight laser scanning system with static calibration

Marcela V. Machado ¹, Antonio M. G. Tommaselli ¹, Thiago T. Reis², Leticia F. Castanheiro ¹, Thaisa A. C. Garcia ¹

Department of Cartography, São Paulo State University (UNESP) at Presidente Prudente, São Paulo, Brazil – (marcela.machado, a.tommaselli, leticia.ferrari, thaisa.correia)@unesp.br
² T2R Technological Solutions, Presidente Prudente, São Paulo, Brazil – tiedtke@gmail.com

Keywords: Static calibration, Lightweight Laser Scanning System, UAV, boresight misalignment.

Abstract

Lightweight aerial laser scanning systems have become a practical alternative over the past few years for collecting 3D geospatial data, typically carried by drones. The positional accuracy expected for the collected data depends on the magnitude of errors generated by the sensors during data acquisition and data processing. These lightweight systems operate in kinematics mode, utilising less accurate attitude sensors compared to conventional aerial systems. Errors resulting from GNSS/IMU solutions (position and attitude) and boresight misalignment angles can significantly affect the accuracy of the point cloud. To reduce errors in platform positioning and other sources of error, a static calibration technique for lightweight systems is proposed in this paper. The technique is based on a static system assembly in a calibration field, using the displacement of a set of specific targets in the object space to simulate a flight path and significantly reduce errors from the positioning and attitude system. This is achieved by levelling the platform using the accelerometers by minimising accelerations in the X and Y axes. The misalignments of boresight angles are estimated based on observations at control points. A technique using the concept of Virtual Control Point (VCP) is also applied to reduce measurement errors. An experimental feasibility study was conducted using a system comprising an IbeoLux laser scanner and a NovAtel SPAN-IGM-S1 inertial measurement unit. The results showed that the technique is viable, but requires some improvements, mainly in using larger ranges. Improvements in boresight estimation were observed when using VCPs, compared to conventional calibration, especially in planimetry.

1. Introduction

The accuracy of lightweight laser scanning systems is affected by various error sources resulting from the combination of measurements from multiple sensors. The investigation of error sources for ALS (Airborne Laser System) has been carried out for many years (Baltsavias, 1999; Schenk, 2001; Skaloud and Litchi, 2006; Habib et al., 2010). Among these errors, special attention should be given to individual sensor calibration, loss of time synchronisation and misalignment between systems (May and Toth, 2007). With lightweight laser scanning systems, error modelling can be more challenging than in ALS systems. Among the critical factors are the low spatial sampling rate and the low number of returns per pulse received by the laser unit, which affects the identification of control entities. In addition, the accuracy of the navigation system is typically lower in lightweight systems, primarily due to errors in the IMU (Inertial Measurement Unit). Thus, considering the errors mentioned, the accuracy of lightweight navigation systems is affected by less accurate sensors and integration failures, which in turn reduce the accuracy of the orientation parameters. Angular misalignment between internal reference systems, which significantly affects overlapping strips, also becomes one of the errors to be modelled. Therefore, calibration procedures are an essential process to eliminate or minimise errors that can affect the positional accuracy of the point cloud (Habib et al., 2010).

Lightweight laser scanning systems have become widely used in applications such as agriculture and forest management; therefore, in-situ calibration based on man-made features is not viable. Another concern is the time spam required for the flight manoeuvres with these systems to enable in-situ calibration. Under these constraints, it is important to optimise the available time, focusing on scanning the object of interest and reducing alignment and calibration manoeuvres. Thus, calibrating the laser scanning system beforehand would be recommended for applications with limited control or man-made features and with

flight time constraints. Therefore, this paper presents a feasibility study of a static calibration approach for lightweight laser scanning systems, with a focus on boresight misalignment angles. This approach aims to minimise errors originating from several sources, such as the position and attitude system, time synchronisation and feature measurement.

2. Lightweight Laser Scanning static calibration

The static calibration of a lightweight laser scanning system was focused on immobilising and levelling the entire system to minimise the position and attitude errors from the GNSS (Global Navigation Satellite System)/IMU integrated unit. The technique is divided into the following steps: (1) assembly of the calibration field; (2) levelling the IMU and the attached laser scanning system; (3) data acquisition and point cloud processing; and (4) determination of boresight angles by least squares adjustment (LSA).

2.1 Assembly of the calibration field

The proposed calibration set-up consisted of two parts: static and mobile (Fig. 1). The static structure was assembled with a metal bar supported by three tripods and poles. The mount with the laser scanning system was attached under the metal bar using four screws, which are used for system levelling. The laser height was determined considering the coverage field over the control targets and horizontal scanning angles, since corners and edges needed to be identified in the laser point cloud without significant occlusions. This structure was maintained static during the data collection procedure. The mobile plate, with dimensions of 1.26 x 1.60 m, was placed over a static supporting plate with 2.50 m x 1.60 m. Four control targets, with trapezoidal prism shape (Fig. 2), were used to simulate objects on the ground with different heights (20 cm and 35 cm) and face orientations (45° and 60°).

The IMU's Y-axis in the static platform was aligned with the north direction to facilitate the determination of the flight path. The same principle of alignment with the north direction is used to position the control targets. The positions of the targets were determined by a GNSS survey of the corners of the fixed plate and trough, using trigonometric relations. The flight simulation is generated by moving the targets in the north direction.

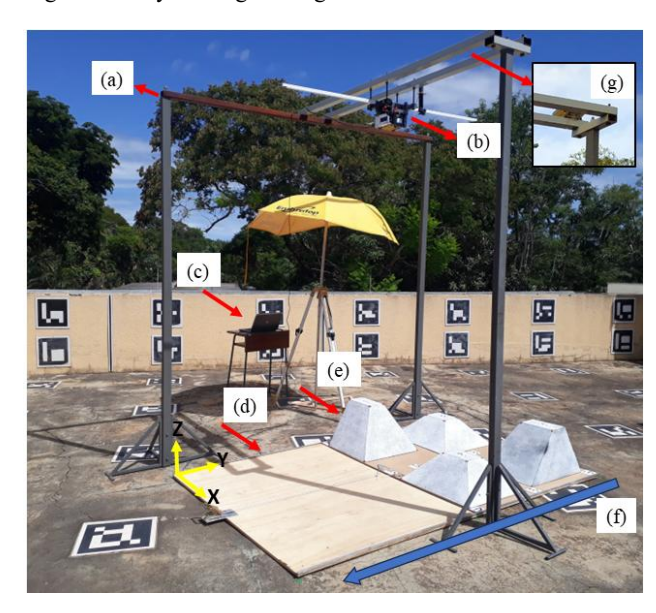


Figure 1. Calibration field: (a) static structure used as system support and levelling, (b) laser scanning system, (c) computer connected to the IMU, (d) mobile ground plate, (e) 3D control targets, (f) direction of mobile plate displacement and (g) GNSS antenna position.



Figure 2. Mobile ground plate: (a) trapezoidal targets and (b) photogrammetric targets.

2.2 System levelling

The system levelling was one of the most important steps in the static calibration procedure. The system orientation provided by the IMU is primarily based on the combined data acquired by gyroscopes and accelerometers, as well as further processing. Considering that these devices are used to measure angular velocities and linear accelerations, two alternatives for levelling can be employed, both utilising information collected from the IMU: real-time monitoring of computed attitude angles (roll, pitch, and heading) or analysing raw data from the accelerometers. As the IMU is considered static, the velocities from gyroscopes can be ignored, and only the accelerations due to the gravity field are provided by the accelerometers. According to Pedley (2013), accelerometers can be used to calculate tilt

angles, but they must be in a static condition, as they are highly sensitive to linear acceleration and the local gravitational field. When levelling using the accelerometers, the X and Y components of the accelerations should be close to zero, and the Z component should be close to 1, considering the use of a scale factor, since the gravitational acceleration should be approximately 9.80665 m/s².

In this case study, the system is levelled in two steps: first, a rough levelling of the system support bars is performed based on a bubble level (Figure 3.a); then, a fine adjustment is made using the screws that connect the payload to the static platform (Figure 3.b). During the fine adjustment, the accelerations of the three axes of the IMU are monitored to bring them as close to zero as possible. A C++ program was developed and implemented by T2R company to display and record the variations of the accelerometers in real time. These variations are shown on the computer screen connected to the inertial system (Figure 3.c). The accelerations are later used to calculate the $R_{IMU}^g(t)$ matrix (Eq. 1).







Figure 3. Laser Scanning levelling: (a) rough levelling with a bubble level, (b) refinement using the system support screws and (c) computer connected to the IMU.

A primary challenge is related to measuring the heading angle since the platform is static and there are no changes in position to enable the kinematics to measure this angle. Since the pitch and roll axes are controlled, an alternative is to physically measure the orientation of the Y-Axis of the IMU by attaching a metal bar aligned with the IMU coordinate system, projecting its endpoints to the ground and measuring these coordinates with GNSS receivers. These endpoints' coordinates are used to calculate the heading/azimuth, to be inserted into the matrix $R^g_{IMU}(t)$. Any movement that affects the heading angle (rotation around the Z-axis) causes a significant effect on the simulated flight, requiring its accurate determination. As it is a critical angle to estimate, a larger error is expected in relation to the tilt angles.

2.3 Data acquisition and processing

The mobile plate was moved over a second supporting plate fixed on the ground in the opposite direction of the expected system flight direction when in kinematic mode. The plate was displaced at fixed lengths. The calculated offsets correspond to half the distance between scanning levels and were obtained based on the vertical scanning angles and laser height. Each offset was associated with four scanning lines. A timestamp was assigned to

each position of the ground plate, and thus to the four scan lines and their corresponding points. This static acquisition technique eliminates any time synchronisation error. Two sets of lever-arm offsets were directly measured with a precision calliper: from the GNSS antenna, and from the laser to the IMU centre. The coordinates of the GNSS antenna were reduced to the IMU centre, and the coordinates of ground points were computed with the raw data with Equation 1 (El-Sheimy et al., 2005; Torres and Tommaselli, 2018).

$$r_{i}^{g} = r_{GNSS}^{g}(t) + R_{IMU}^{g}(t)r_{LU}^{IMU} + R_{IMU}^{g}(t)R_{LU}^{IMU}R_{ED}^{LU}(t)\rho_{I}$$
 (1),

in which (r_i^g) are the ground coordinates of a point i; $r_{GNSS}^g(t)$ are the ground coordinates of the GNSS antenna at instant t, reduced to the IMU coordinate system; $R_{IMU}^g(t)$ is the rotation matrix relating the ground and IMU coordinate systems at instant t, derived after processing the GNSS and IMU data; r_{LU}^{IMU} are the offsets between the laser unit and IMU origin (lever-arm); R_{ED}^{LU} is the rotation matrix relating the laser emitting device with the laser unit coordinates system at instant t, as a function of the mirror scan angles β and θ ; (ρ_I) is the range; R_{LU}^{IMU} is the rotation matrix that relates the laser unit and IMU coordinate systems, the boresight\angles $(\Delta \kappa, \Delta \varphi, \Delta \omega)$.

In this proposed method, roll and tilt angles should be null due to the mechanical levelling of the platform. However, differential movements of the platform may still occur. To avoid these errors, the accelerometer measurements were used to calculate these angles.

2.4 Boresight determination with point-based approach

The boresight misalignment angles are critical parameters because even small angular variations can significantly impact point cloud accuracy, depending on the flight height (May, 2008). In this paper, these parameters are estimated based on control points measured both in the point cloud and on the ground. Two approaches were considered: (1) discrete point identification in the point cloud, and (2) Virtual Control Point (VCP). The estimation of boresight angles based on the discrete point approach will be affected by the measurement error, considering that a point identified in the point cloud does not correspond rigorously with the control point determined in the field. Using the VCP technique (Machado and Tommaselli, 2023) can minimise these errors. In this technique, the coordinates of the apex points (vertex) are obtained by the intersections between planes (faces) of the trapezoidal control target. Since the apex points are virtual points and thus do not have raw data, it is necessary to find the nearest neighbour points that have this data.

The equation of the laser mathematical model (Equation 1) can be rearranged (Torres and Tommaselli, 2018) to obtain Equation 2, which serves as the basis for estimating the boresight angles.

$$R_{IMU}^g(t)^{-1} * [r_i^g - r_{LS}^g(t)] = R_B R_{LU}^{IMU} r_i^{LU}(t)$$
 (2),

$$r_{LS}^g = r_{GNSS}^g(t) + R_{IMU}^g(t) r_{LU}^{IMU}$$
 (3),

$$r_i^{LU}(t) = R_{ED}^{LU}(t)\rho_i(t) \tag{4},$$

in which: r_{LS}^g is a vector of coordinates of the centre of the laser unit in the ground reference system; $r_i^{LU}(t)$ is the 3D position of point i in the laser unit reference system, computed by Equation (4); R_B is introduced as the matrix of the unknown parameters (boresight angles $-\Delta\omega$, $\Delta\varphi$ e Δk). R_{LU}^{IMU} is now used as a constant matrix, to make the laser unit systems compatible

with the IMU, with the fixed elements: $\Delta \kappa = 0^{\circ}$, $\Delta \varphi = -90^{\circ}$, and $\Delta \omega = 90^{\circ}$.

The estimation of the boresight angles can be performed with the Gauss-Legendre Least Squares adjustment, by considering the left term of Equation 2 $(R_{IMU}^g(t)^{-1} * [r_i^g - r_{LS}^g(t)])$ as the observation. Since the variance of the observations is considered the same, the weight matrix can be assumed to be the identity. This option is quite simple, but it does not consider the individual errors in the observations.

A second option is to use a combined method of adjustment (Gauss-Helmert – Wells and Krakiwsky, 1971), which handles observations and parameters. This model enables the treatment of a larger number of elements as observations for estimating unknowns, as outlined in Equation 5. With such approach, the determination of the boresight angles must consider six observations: the control point coordinates $(X_{GCPi}, Y_{GCPi}, Z_{GCPi})$, the scanning angles $(\theta \in \beta)$ and the range (ρ) .

Rearranging the basic mathematical model presented in Equation 2 to meet the conditions of the combined method leads to Equation 5.

$$R_{IMII}^g(t)^{-1} * [r_i^g - r_{IS}^g(t)] - R_B R_{UL}^{IMU} r_i^{UL}(t) = 0$$
 (5)

Thus, the two estimation techniques were applied to compare their performance in the context of terrestrial calibration. Additionally, the techniques are applied both with and without the use of the VCP methodology. The description of the models is presented in Machado and Tommaselli (2023) for the aerial case, being adapted in this work for the terrestrial case. Both approaches consider that the raw data are available from the system, such as position, attitude, data from the GNSS/IMU system, angles and ranges measured by the laser scanning unit.

3. Experiments and results

3.1 Assessment of the calibration field and levelling

Initially, experiments were conducted using the Ibeo LUX scanner to evaluate the accuracy of the range measurements and determine the optimal characteristics for the control targets and calibration field. Results indicated an accuracy close to that specified by the manufacturer, which is approximately 4 cm. The estimated root mean square error (RMSE) of the assessed ranges was approximately 0.035 m and 0.052 m for experiments with distances of 0.6 m and 1.5 m, respectively. These ranges were tested to design the laser height in the calibration field. However, the range was increased since the initial experiments for short ranges presented a circular effect in the point cloud, similar to the smile effect described by Morin (2002). This effect was not a systematic error, but rather a random effect of the laser time discretisation used to compute the range. Therefore, the range or height of the laser unit in relation to the ground was set to 2.45 m, also enabling better coverage of the control targets. The static structure was set to approximately 3 m from the ground, considering the laser unit height.

The structure of the acquisition platform was previously aligned northward. To assess the platform alignment, six control points were surveyed (four points at the ends of the fixed plate and two points in the centre, corresponding to the ends of the mobile plate). GNSS receivers were used to survey the control points, achieving an accuracy of 3 mm. From these coordinates, the azimuth of the fixed plate was calculated.

The values of the incremental movement steps of the plate with targets were used to generate the coordinates of a simulated flight trajectory. The initial coordinates were obtained by translating the centre of the GNSS antenna to the origin of the IMU, taking into account the lever arm. The heading angle was estimated by projecting the IMU Y axis (North oriented) to the plate, achieving a value of $-05^{\circ}06^{\circ}16.2^{\circ}$. The determined angle was applied to the matrix $R_{IMU}^g(t)$, to correct the orientation of the point cloud.

The selection of raw data packets collected by the laser unit was performed using a C++ script developed in QT Creator. Since the laser emits several pulses continuously, generating numerous data packets, a plate was placed between the sensor and the control targets for a few seconds, in order to separate the packets by displacement instant (position). For each set of packets obtained based on the displacement, only one was used to generate the point cloud. Thus, a total of 163 packets (652 scan lines) were stored, which corresponds to the number of displacements and, consequently, the number of acquisition stations.

After data acquisition and selection, it was necessary to synchronise the laser scan data with the data provided by the IMU. This could not be done in real time due to the characteristics of the acquisition made for this experiment. The synchronisation was performed based on their correspondence with the raw data during the acquisition. Since the variations in the accelerations were stored in the computer, they were grouped into eight sets and used to generate the point cloud. Synchronisation associated the data from sensors using GPS time as a label. The accelerations of each axis were normalised, and the roll and pitch angles were calculated from the accelerations (Pedley, 2013). The heading angle was obtained as previously described. To identify which scan line contains a control point, it was necessary to generate an initial point cloud and visualise it in the Cloud Compare software, together with the control points. For each control point, an approximate corresponding point was identified in the point cloud. The data package corresponding to the scan line of interest was identified in the raw data file through the approximate coordinates of the point. From the package identifier, the start and end time of this package was verified.

The acquired data was used to generate the point cloud with Equation 1. For each generated scan line, the proximity to a control point was verified. After identifying this proximity to the control, the values of the rotation matrix $R_{IMU}^g(t)$, calculated from the accelerations measured by the accelerometers, were used.

3.2 Boresight angles determination

The estimation of angular misalignment for the terrestrial case was performed and evaluated for two groups of experiments (Table 1) using control points. Group 1 included the steps: (1) interactive/manual selection of the nearest neighbours to the point of interest in the point cloud; (2) point-based estimation (Gauss-Legendre and combined method); (3) quality control. Group 2 included: (1) determination of the virtual control points (VCP) based on the faces of each target (Machado and Tommaselli, 2023); (2) selection of the nearest neighbours to the VCP in the point cloud (3) point-based estimation (Gauss-Legendre and combined models); (4) quality control. It is worth noting that the experiments were conducted in a local coordinate system to avoid numerical issues.

Regarding Group 1, for each ground control point, the closest corresponding points in the laser point cloud were identified. A

radius of approximately 5 cm was manually applied using the Cross Section (Cloud Compare) tool to filter the points of interest in the cloud; subsequently, only four points closest to the control point were selected. Since time is used as a label when generating the raw point cloud, this value was extracted after selecting the coordinates of the points of interest. Using this timestamp, the raw data (scan angles, distance, position, and attitude) corresponding to the points of interest were identified in the point cloud processing file without correction. These data (control point coordinates, simulated flight path coordinates, attitude angles, horizontal scan angle, vertical scan angle and range) were used as input to estimate the boresight angles. From a total of 32 ground control points, 14 were used in the estimation of the boresight angles, and the remaining were used as check control for quality control.

Exp.	Procedure				
G1	Α	No correction			
	В	Boresight correction based on Gauss-Legendre Method			
	С	Boresight correction based on Combined Method			
G2	D	No correction - with PCV			
	Е	Boresight correction based on Gauss-Legendre Method with VCP			
	F	Boresight correction based on Combined Method with VCP			

Table 1. Characteristics of the experiments.

Regarding the adjustment trial with the combined method, the following standard deviations were used to calculate the weight matrix: σ_{X_GCP} , σ_{Y_GCP} , $\sigma_{Z_GCP} = 0.01$ m; $\sigma_{A\theta} = 2.424 \times 10^{-4}$ rad; $\sigma_{A\beta} = 4.848137\times 10^{-7}$ rad; $\sigma_{A\rho} = 0.04$ m. The standard deviations of the control point coordinates were determined based on the expected measurement error for these points, considering that the points were surveyed with millimetre precision. The value assigned to the standard deviation of the range was provided by the manufacturer. The accuracy of the scanning angles was estimated empirically based on the step size of the servomotor of the laser unit. The processing solution converged after six iterations.

Group 2 of experiments were performed using the concept of VCPs. To improve the identification of the laser point, homologous to the control point, the faces of each trapezoidal target were cropped with Cloud Compare. For each face, composed of n laser points, a plane was adjusted using the *fitplane* tool implemented in Octave software. Outliers were removed by iteratively analysing the distances between the cloud points and the generated planes, with a threshold of 6 cm. Then, the point of intersection of the three planes was calculated for each corner of the trapezoidal targets, resulting in 32 apex points, which were obtained as a function of the four control targets. After calculating the coordinates of the apex points of the targets in the clouds, these points were used as a reference for collecting the closest neighbouring points belonging to the point cloud, as was done in the experiments of Group 1.

The raw data of the points of interest (nearest neighbours) were obtained through the time stamp. The weights adopted for the algorithm remained the same as in the experiments of Group 1. Since the apex points are generated through plane adjustment, they do not have raw data, and therefore, it is necessary to collect the closest neighbouring points. In this regard, for each of the 32 vertices coming from the targets of the mobile platform, 4 neighbouring points with raw data information were collected,

totalling 128 points. Figure 4 shows the distribution of the apex points calculated with the plane adjustment. Even after removing outliers, the effect caused by the laser range error still affected the adjustment of some plane faces, and consequently, the determination of the apex point. This resulted in the removal of some points used to determine the boresight angles (discarded points). A total of 21 points (with 75 neighbouring points in the cloud) were used to estimate the boresight angles, and 7 points were used for quality control. Since the acquisition was performed in only one direction, there is only one flight simulated direction.



Figure 4. Distribution of apex points in the point cloud: (a) yellow – points for calculating boresight angles; (b) green – points for quality control, and (c) red – discarded points.

3.3 Static calibration - Quality control

A set of boresight angles and their respective standard deviations were estimated and subsequently applied to correct the points selected for quality control. Table 2 presents the set of angles obtained for Groups 1 and 2. Considering the two distinct methods evaluated, the residuals were consistent with the standard deviations of the observations.

			. /=\ /=\		
Exp.		$\Delta\omega(^{\circ}) \pm \sigma\omega(^{\circ})$	$\Delta \varphi(^{\circ}) \pm \sigma \varphi(^{\circ})$	$\Delta \kappa(^{\rm o}) \pm \sigma \kappa(^{\rm o})$	
G1	Α	1	1	-	
	В	$0.5433 \pm$	$0.2922 \pm$	0.9147	
		0.1094	0.1056	± 0.5306	
	С	$0.5361 \pm$	0.2903 ±	0.9853	
		0.0800	0.0775	± 0.3872	
G2	D	1	1	1	
	Е	$0.5383 \pm$	$0.2822 \pm$	0.6447	
		0.1097	0.1058	± 0.5319	
	F	$0.5319 \pm$	$0.2794 \pm$	0.7081	
		0.0781	0.0753	± 0.3775	

Table 2. Boresight angles estimated and standard deviations – Groups 1 and 2.

Regarding the evaluation of the effects of the correction of boresight angles estimated (Table 2) on point clouds, the results of the quality control are summarised in Table 3. The standard deviation and RMSE for experiments A to C were calculated based on 7 checkpoints, evenly distributed throughout the area of interest. Comparing A with B and C, slight improvements were observed, with variations found in the order of millimetres. Considering the standard deviation, the same precision is maintained for both experiments. Only the N component

presented better results after the corrections, as analysed by the RMSE. In contrast, the E component maintained the same accuracy, while the h component presented a difference of approximately 1 mm. Regarding the boresight angle estimation techniques, the results of Group 1 using the Gauss-Legendre method (B) were similar to those of the combined method (C), after applying the correction for boresight angles, particularly in planimetric coordinates.

Exp.		Standard Deviation (m)			RMSE(m)		
		ΔΕ	ΔN	Δh	ΔΕ	ΔN	Δh
G1	A	0.027	0.010	0.021	0.046	0.046	0.032
	В	0.030	0.008	0.039	0.046	0.045	0.031
	С	0.030	0.008	0.039	0.046	0.044	0.031
G2	D	0.026	0.017	0.022	0.043	0.043	0.036
	Е	0.028	0.002	0.037	0.044	0.040	0.035
	F	0.028	0.002	0.037	0.044	0.040	0.035

Table 3. Quality control: comparison between Groups 1 and 2.

The planimetric errors at the checkpoints for Experiments D and F are shown in Figure 5. The discrepancies are randomly distributed, and variations can be noted depending on the position of the points (low-right area). Affecting the final statistics, such as the RMSE. The reasons for the error distributions were not determined in these experiments.

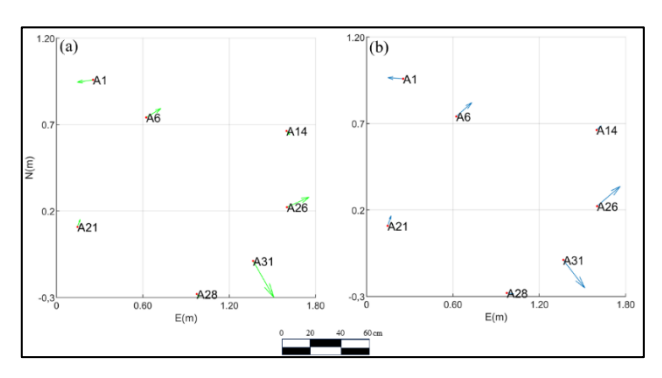


Figure 5. Planimetric discrepancies according to flight direction: (a) Experiment D and (b) Experiment F.

Considering the results of the techniques used in Group 1 of experiments, the VCP technique was applied in Group 2 (D to F). When comparing experiment D with experiments E and F, the same behaviour of results found in group 1 is observed. When analysing experiments E and F, in which boresight angles are estimated from VCP, with experiments B and C, an improvement in planimetry (approximately 2 and 6 mm, respectively) and a worsening in altimetry (approximately 4 mm) are observed. These results indicate that the initial point cloud was accurate and that the errors caused by angular misalignment are small for this laser-object distance, being of the same magnitude as the random errors, for both the experiments of Group 1 and Group 2. However, the VCP technique can be considered a viable alternative. Figure 6 shows the final point cloud generated from the data collected in the calibration field.

It can be concluded that the measurement errors affected the estimation of the boresight angles, leading to a precision that was not sufficient to perform the expected corrections of the point cloud. This happened most likely due to the short distance (2.45 m) used in the data acquisition.

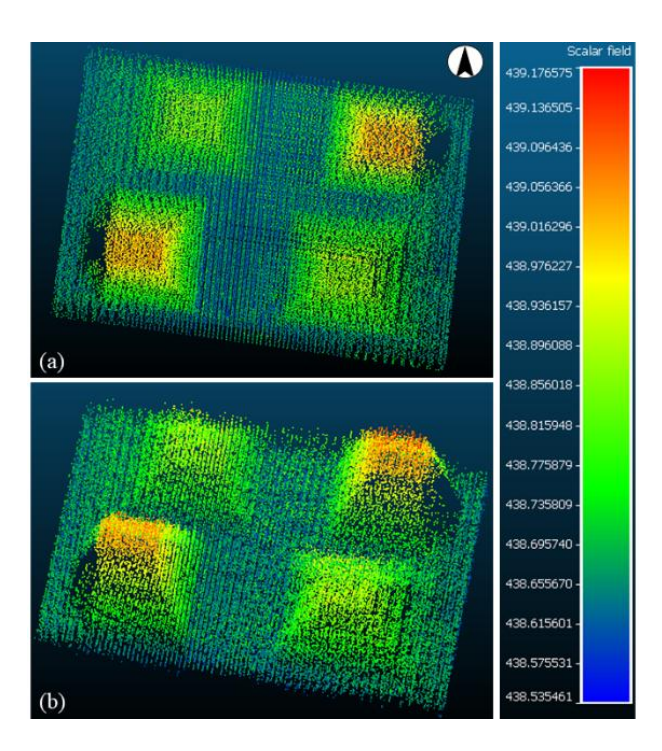


Figure 6. Point cloud obtained in static calibration: (a) top view; and (b) three-dimensional view of the point cloud.

4. Conclusions

The initial results of this feasibility study indicate that static calibration is a viable alternative for estimating boresight misalignment angles as it enables reducing errors caused by the attitude and positioning system, and time synchronisation. Levelling the system while observing the accelerometers was effective in reducing and estimating tilt angles. The technique is an option for system calibration in applications such as forest and agricultural mapping, where it is challenging to find man-made features to use with in-situ calibration. However, in this static technique, the measurement of heading angle still requires more improvements. One alternative is to leave the refinement of this value as a parameter for *in-situ* determination. It is also necessary to study the effects of using further strips in different directions and heights.

Regarding the features to be measured for boresight angle determination, the use of control points provided good results compared to other works; however, it is still less accurate than some approaches that utilise primitives such as lines and planes. Furthermore, the smile-like effect, caused by an error in range measurement, had a clear noise effect on the point cloud. Even considering those drawbacks, it was shown that close-range and static calibration is viable. Including more sources of control, such as planes and lines, is recommended for future work. The primary change in the calibration setup should be the use of a larger range, which will help to reduce the effects of range error in the estimation process. This solution would be feasible by modifying the design adopted for this calibration field by orienting the scanner horizontally, rather than vertically, as performed in the experiments, to test different distances more easily. In conclusion, the structure requires modifications; however, the initial results were promising, making this static calibration technique a viable alternative for both lightweight aerial scanning systems and terrestrial mobile mapping systems.

Acknowledgements

This study was financed in part by the São Paulo Research Foundation, FAPESP (2021/06029-7), Coordenação de Aperfeiçoamento de Pessoal de Nível Superior – CAPES (Grant: 88882.433955/2019-01), and Conselho Nacional de Desenvolvimento Científico e Tecnológico - CNPq (Grant: 141550/2020-1).

References

Baltsavias, E. P., 1999. Airborne laser scanning: basic relations and formulas. ISPRS Journal of Photogrammetry and Remote Sensing, v. 54, n. 2–3, pp. 199–214.

El-Sheimy, N.; Valeo, C.; Habib, A., 2005. *Digital Terrain Modeling: Acquisition, Manipulation and Applications*, Artech House, Norwood, Massachusetts, 257 p.

Habib, A.; Bang, K. I.; Kersting, A. P.; Chow, J., 2010. Alternative methodologies for LiDAR system calibration. Remote Sensing, v. 2, n. 3, p. 874-907.

Machado, M. V.; Tommaselli, A. M. G., 2023. UAV-LIDAR boresight estimation using virtual control points: a case study. ISPRS Annals of the Photogrammetry, Remote Sensing and Spatial Information Sciences, v. X-1/W1-2023, pp. 1073-1080

May, N. C.; Toth, C. K., 2007. Point Positioning Accuracy of Airborne LiDAR Systems: A Rigorous Analysis. International Archives of the Photogrammetry, Remote Sensing and Spatial Information Sciences, v. 36, n. 3, pp. 19-21.

Morin, K. W., 2002. *Calibration of Airborne Laser Scanners*. Doctoral Dissertation, University of Calgary, Calgary.

Pedley, M., 2013. Tilt sensing using a three-axis accelerometer. *Freescale semiconductor application* note, 1, 2012-2013.

Schenk, T., 2001. Modeling and recovering systematic errors in airborne laser scanners. Proceedings of OEEPE Workshop on Airborne Laserscanning and Interferometric SAR for Detailed Digital Terrain Models.

Skaloud, J.; Lichti, D., 2006. Rigorous approach to boresight self-calibration in airborne Laserscanning. *ISPRS Journal of Photogrammetry and Remote Sensing*, v. 61, n. 1, p. 47-59.

Torres, F. M. and Tommaselli, A. M. G., 2018. A lightweight UAV based laser scanning system for forest application. *Bulletin of Geodetic Sciences*, 24(3), 318-334.

Wells, D.E., Krakiwsky, E.J., 1971. The Method of Least Squares. *Department of Geodesy and Geomatics Engineering University of New Brunswick*, Canada.